Technical Note:

A note on small-scale potential feedback mechanisms of large-scale ocean circulations

by Hans van Haren

Royal Netherlands Institute for Sea Research (NIOZ), P.O. Box 59, 1790 AB Den Burg, the Netherlands.
e-mail: hans.van.haren@nioz.nl

Short summary. The extent of mankind's influence on Earth's climate warrants ocean-studies. A supposed major heat-transporter is the Atlantic Meridional Overturning Circulation (AMOC). As AMOC is a complex nonlinear dynamical system, mathematical models may predict its potential collapse using single parameters like surface temperature. However, physical processes such as (sub-)mesoscale eddy transport and turbulent mixing by internal wave breaking will alter the estimators, so that the AMOC may not collapse.

Abstract. The extent of anthropogenic influence on the Earth's climate warrants studies of the ocean as a major player. Large, basin-wide ocean circulations are important for transporting properties like heat, carbon and nutrients. A supposed major conduit is the Atlantic Meridional Overturning Circulation (AMOC). As the AMOC is a complex nonlinear dynamical system, it is challenging to predict its potential to collapse and/or reversal of direction from a statistical viewpoint using a single parameter like sea-surface temperature or freshwater influx in numerical models. However, as is argued in this note supported by spectra from ocean observations, small-scale physical processes such as, for example, transport by sub-mesoscale eddies and turbulence-generating breaking of internal waves that are not incorporated in these models will alter such parameters, and thereby statistical analyses. This may lead to feedback mechanisms on property gradients such as density stratification so that large-scale ocean circulations like the AMOC may not collapse.

1 Introduction

Schematically, the Atlantic(-Ocean) Meridional Overturning Circulation (AMOC) is depicted to transport heat from the equator to the poles near the surface and carbon in the abyssal return (e.g., Aldama-Campino et al., 2023). It includes physical processes like 'deep dense-water formation' in the polar region. Recent mathematical and numerical modelling such as based on varying single parameters like sea-surface temperature (e.g., Ditlevsen and Ditlevsen, 2023) and freshwater influx (e.g., van Westen et al., 2024) suggest a potential

59 future collapse of the AMOC. It is argued that this may have consequences for Northwest-
60 European climate.

61 Whilst the modelling might be robust mathematically, it lacks physical processes of
62 the drivers of the AMOC and observational evidence thereof. This will have consequences for
63 the feedback mechanisms at work in the nonlinear dynamical system of ocean circulation. As
64 has been reviewed for AMOC numerical models (Gent, 2018), important feed-back
65 mechanisms are vertical (turbulent) mixing, (sub-)mesoscale gyre (eddy) transport, and the
66 coupling with the atmosphere. Here we elaborate on the importance of turbulence induced by
67 internal wave breaking, possibly coupling with sub-mesoscale eddies, and stability variations
68 in vertical density stratification for such feed-back, by reviewing insights from recent
69 modeling and deep-sea observations. In particular, the core of ocean motions is spectrally
70 investigated focusing on most energetic mesoscale, internal wave, and turbulence scales.

71 In contrast with the atmosphere, the ocean is not an ineffective heat engine (Wunsch
72 and Ferrari, 2004) despite its heat transportation. As a result, the AMOC is not predominantly
73 buoyancy-driven via push by deep dense-water formation near the poles (Marshall and Schott,
74 1999; Marotzke and Scott, 1999), which notably occurs in sporadic pulses rather than
75 continuously. Instead, the AMOC is mainly wind- and tide-driven, with turbulent mixing by
76 internal wave breaking, and possibly associated upwelling close to boundaries (Ferrari et al.,
77 2016), being considered an important physics process of pull that dominates over push by a
78 heat engine. Winds, near the ocean surface, and tides, via interaction with seafloor topography
79 deeper down, contribute about equally to generate internal waves that are found everywhere
80 in the ocean interior. Such waves break predominantly at ubiquitous underwater seamounts
81 and continental slopes.

82 Without turbulent mixing, the AMOC would be confined to a 100-m thick near-
83 surface layer and the deep-ocean would be a stagnant pool of cold water (Munk and Wunsch,
84 1998). This is not the case however, and the solar heat is mixed from the surface downward
85 so that the ocean is stably stratified in density all the way into its deepest trenches, as has been
86 shown in hydrographic deep-ocean observations (Taira et al., 2005; van Haren et al., 2021a).

Although turbulent mixing by internal wave breaking in the ocean-interior is insufficient by at least a factor of two to maintain the vertical density stratification (e.g., Gregg, 1989, Polzin et al., 1997), such breaking along ocean boundaries has been suggested to be more than sufficient (Munk, 1966; Polzin et al., 1997). Especially large internal wave breaking is expected to occur above steeply sloping topography (Eriksen, 1982; Thorpe, 1987; Sarkar and Scotti, 2017). Because there are more and larger seamounts than mountains on land, equally abundant sloping seafloors lead to abundant turbulent mixing, as has been charted from recent observations and modelling results summarized below.

2 Recent internal wave breaking results

Detailed observations and numerical modeling have revealed the extent of internal tide breaking processes above ocean topography (van Haren and Gostiaux, 2012; Winters, 2015; Wynne-Cattanach et al., 2024). Quantification of the turbulent mixing shows that it occurs with typical tidal-period-average values that are more than 100 times larger over (just) super-critical slopes than open-ocean values. A super-critical seafloor slope is steeper than the slope of internal wave characteristics. While ocean-wide tides energetically dominate internal waves, not all seafloor slopes are super-critical for these waves. In contrast, nearly all seafloor slopes are super-critical for (at least one component of) secondly energetic near-inertial waves, which are generated via geostrophic adjustment following the passage or collapse of a disturbance such as fronts or atmospheric storms on the rotating Earth. Under common stratification, near-inertial waves are at the lowest frequency of freely propagating internal waves. The highest frequency propagating internal waves, near the buoyancy frequency, experience only vertical walls as super-critical seafloor slopes.

Within a tidal, or near-inertial, period, turbulence peaks in bursts of shorter duration than half an hour when highly nonlinear internal waves propagate as internal bores up a super-critical slope, once or twice a tidal cycle. The breaking of bores leads primarily to convective, buoyancy-driven turbulence, rather than frictional shear-turbulence over the sloping seafloor and occur at a wide variety of deep-sea and deep-ocean locations (e.g., van

Haren et al., 2013; van Haren et al., 2024). Between bores, the turbulent mixing varies by an order of magnitude in intensity, with effects extending about 100 m vertically and several kilometers horizontally from the seafloor. Although intermittently occurring at a given position of the sloping seafloor and about 10% varying in arrival time, the turbulence is generated internally by the tide, for about 60% (Wunsch and Ferrari, 2004), and by winds, for about 40%, in a stratified ocean-environment. The turbulent bores also resuspend sediment and thereby replenish nutrients away from the seafloor (Hosegood et al., 2004), important for deep-sea life. Enhanced turbulent mixing above (sloping) boundaries has a demonstrated effect on the outcome of general ocean circulation models (e.g., Scott and Marotzke, 2002), with predicted subtle effects on upwelling near the seafloor (Ferrari et al., 2016).

The question is whether the intensity of internal-wave induced deep-ocean turbulence is affected by variations in sea-surface temperature or salinity, with what consequences for the AMOC. In considering these it should be noted that various properties determine different equilibria. For example, deep dense-water formation does not only occur in polar seas, but occasionally also in the at least 10°C warmer Mediterranean (Gascard, 1978), with an important contribution of atmospheric exchange due to orographic generated winds affecting the preconditioning by cooling and drying of near-surface waters. Similarly, internal waves occur in oceans and in the Mediterranean under stratification conditions that vary over at least of magnitude in time and space, but tides are relatively weak in the Mediterranean, and yet 'sufficient' turbulent diapycnal mixing, sufficient for maintenance of deep-sea stratification and thereby driving overturning circulation, is generated via (the breaking above topography of) near-inertial motions mainly (van Haren et al., 2013). Further complications are expected from interactions of internal waves with (sub-)mesoscale eddies and potential consequences of varying intensity thereof, e.g., on seasonal scales.

3 Mediterranean observations as an example proxy for ocean conditions

In many physical oceanographic aspects of heat and salt budgets, large-scale water-flow circulation, strong boundary flow, eddies at sub-mesoscales, near-inertial motions

143 including gyroscopic waves and internal wave turbulence, the Mediterranean Sea can be
144 considered a sample for the state of the much larger oceans (e.g., Gascard, 1973; Crepon et
145 al., 1982; Garrett, 1994; Milllot, 1999; van Haren and Millot, 2004; Testor and Gascard,
146 2006). Like in oceans, the Mediterranean seafloor reaches great depths and can be rugged
147 with steep slopes in places, including continental slopes incised by deep canyons.

148 In the Northwest Mediterranean, vertical density stratification varies markedly with
149 seasons and years, having relatively large near-surface values in summer and relatively low
150 values in winter. The proximity of extensive mountain ranges on land generates highly
151 variable winds that can cool and dry surface waters. In winter in weaker stratified waters, this
152 may lead to unstable conditions of buoyancy driven convection in an exchange of dense-water
153 sinking down, and less dense-waters up. Like in the polar regions, such exchange can be
154 observed daily in the upper 10 m from the sea-surface, regularly down to a few 100 m from
155 the surface, and seldom, once every 5-8 years (e.g., Rhein, 1995; Mertens and Schott, 1998),
156 down to the abyssal seafloor at about 2500 m. In contrast, horizontal density gradients
157 associate with forcing of a dynamically unstable boundary current and eddies at multiple 1-
158 100 km (sub-)mesoscales (e.g., Crepon et al., 1982; Testor and Gascard, 2006). These eddy
159 motions may push relatively warm waters down, thereby increasing the weak stratification in
160 the deep-sea.

161 In summer, atmospheric disturbances are less intense, near-surface stratification is
162 large due to solar heating, and eddy activity associated with some continental boundary flows
163 is weaker (Albérola et al., 1995). This opens the possibility for detection of near-inertial wave
164 dominance in kinetic energy. In relatively strong stratification, mainly gravity-driven parts of
165 near-inertial waves generate largest vertical current differences ‘shear’ that destabilize
166 stratification due to their relatively short vertical length-scale, not only in the Mediterranean
167 but also as observed in the Atlantic Ocean (van Haren, 2007). This destabilization may lead to
168 small-10-m vertical scale layering of near-homogeneous waters throughout seas and oceans.
169 On larger-100-m vertical scales near-homogeneous waters occur in deep waters of the
170 Mediterranean as well as of North-Atlantic basins like the Bay of Biscay and Canary Basin.

In near-homogeneous water-layers with weak stratification, gyroscopic, Earth-rotation-driven, parts of near-inertial waves dominate and result in 0.1-1 km diameter sub-sub-mesocale tubes of slantwise rather than vertical convection (Emanuel, 1994; Marshall and Schott, 1999; van Haren and Millot, 2004). Hence, one may expect frequency spectra of non-tidal dominated data from instruments moored in the Mediterranean reveal convection and thus deep transport under winter and summer conditions.

It is noted that ocean-spectra may show peaks such as at narrowband tidal and at, broader band, inertial frequencies, but they lack gaps. This lack of spectral gaps potentially couples motions at sub-inertial with inertial-buoyancy internal wave with super-buoyancy turbulence frequency ranges. However, it is unclear how such a coupling may work as some motions represent two-dimensional (2D) eddies, some linear waves, some non-linear waves, some anisotropic stratified turbulence, and some isotropic 3D turbulence. This is investigated by re(newed) spectral analysis below, using, in analogy, slopes typical for investigating energy cascades in turbulence research.

4 Uncommon slopes in revisited spectra

Kinetic energy (KE) spectra from historic moored current meter observations down to mid-depth z = -1100 m in the Ligurian Sea under upper-sea strongly stratified 'summer' and weakly stratified 'winter' conditions surely lack gaps (Fig. 1). Although these hourly sampled data barely resolve the turbulence ranges at frequencies higher than the buoyancy frequency, the internal wave continuum was suggested to scale with frequency ω like ω^p, with, on a log-log plot, 'spectral slope' $p = -2.2 \pm 0.4$ (van Haren and Millot, 2003), independent of location and season albeit with different KE (power) levels.

Within the uncertainty range, several possible explanations can be given for the observed spectral slope. Internal gravity waves have been fitted to $p = -2 \pm 0.5$ but only for $f << \omega << N$ (Garrett and Munk, 1972), where f denotes the inertial frequency involving Earth rotation and N denotes the buoyancy frequency reflecting the square-root of vertical density

198 stratification. Considering that the data in Fig. 1 are from a site where locally N = (3±2)f,
199 irrespective of season (van Haren and Millot, 2003), alternative explanations were sought for
200 observed spectral slopes at sub-inertial frequencies 0.2 cpd < ω < f. Cpd is short for 'cycles
201 per day'. An obvious candidate is 'fine-structure contamination' of step functions passing
202 sensors which gives a theoretical vale of p = -2 (Phillips, 1971; Reid, 1971). For their winter
203 data, van Haren and Millot (2003) attributed such a slope to evidence intense mesoscale
204 activity, because of the continuation of slope up to ω = 5 cpd before rolling off to white noise
205 (slope 0). However, they did not elaborate. Below, the data in Fig. 1 are re-analyzed from the
206 perspective of convection-turbulence.

207 Theoretical considerations of non-zero-mean flow convection-turbulence suggest a
208 spectral scaling in the buoyancy range having p = -11/5 = -2.2 for KE, and p = -7/5 for a(n
209 active) scalar quantity. This 'BO'-scaling follows atmospheric and theoretical works by
210 Bolgiano (1959) and Obukhov (1959). The scaling was set-up for a stably stratified
211 (atmospheric) environment for the anisotropic part in which turbulent kinetic energy is
212 partially transferred to potential energy leading to turbulent convection. Later works extended
213 BO-scaling to purely buoyancy-driven turbulence, e.g., for Rayleigh-Bénard convection
214 (Lohse and Xia, 2010).

215 Laboratory experiments on such gravitationally driven convection are inconclusive on
216 BO-scaling. This scaling is confirmed for both KE and temperature in experiments by
217 Ashkenazi and Steinberg (1999), while only for scalars by Pawar and Arakeri (2016) who
218 found a slope of p = -5/3 for KE. The p = -5/3-slope suggests dominance of shear-induced
219 turbulence of the inertial subrange for equilibrium (isotropic) turbulence cascade in the 'KO'-
220 scaling (Kolmogorov, 1941; Obukhov, 1949) but should also be found in spectra of scalars
221 that are passive in this range. Obviously, scalars cannot be passive and active at the same time
222 and in the same space. This discrepancy between (types of) scaling between scalars and KE
223 may be because the laboratory experiments of Pawar and Arakeri (2016) were in zero mean
224 flow. Also, under sufficiently stable conditions without shear, no inertial subrange is expected

(Bolgiano, 1959). However, the spectral extent of BO-scaling is largely unknown albeit it is more generally found adjacent to higher-frequency inertial subrange. While KO-scaling is based on a forward cascade of energy, the direction of energy cascade is inconclusive for BO-scaling and may be partially forward and partially backward, at least as reasoned for pure buoyancy-driven convection-turbulence (Lohse and Xia, 2010). Probably, directions of cascade change with locality in the flow, and perhaps depend on scale, which would also imply that KO- and BO-scaling cannot be found at the same site.

Revisiting data from non-zero mean flow and (weakly) stratified deep-sea in Fig. 1 demonstrates the possibility of fit of $p = -11/5$ outside near-inertial harmonic peaks. In winter, such a fit is observed consistently through the entire range of $0.2 < \omega < 5$ cpd. In traditional terms, this frequency range covers the transition from mesoscale $\omega < f$, via internal wave $f < \omega < N$, to turbulence $\omega > N$ motions. In summer, the $p = -11/5$-slope is found at two different KE levels for bands $0.2 < \omega < \omega_{min}$ and $2\Omega < \omega < 5$ cpd at sub- and super-IGW frequencies, respectively. Here, $\omega_{min} < f$ denotes the minimum frequency bound for inertio-gravity waves IGW (LeBlond and Mysak, 1978), and Ω the Earth rotational frequency. Maximum IGW frequency is denoted by $\omega_{max} > 2\Omega$. The plotted IGW-bounds $[\omega_{min}\ \omega_{max}]$ are for weakly stratified, near-homogeneous layers in which $N = f$.

The bridge between the KE-levels at sub- and super-IGW is formed by the finitely broad near-inertial peak. The base of this peak is proposed to slope like $p = -1$ reaching super-IGW BO-scaling at about $\omega \approx 4$ cpd $\approx N$. Such $p = -1$-slope has been observed for the KE-spectral continuum between $[f\ N]$ from the deep Bay of Biscay, Northeast Atlantic Ocean (van Haren et al., 2002). Theoretically, this slope represents spectral scaling of intermittency of a weakly chaotic nonlinear system (Schuster, 1984), i.e., 3D dynamical systems that evolve into self-organized critical structures of states which are minimally stable (Bak et al., 1987). Such a spectral bridge, or hump, is expected for turbulence in unstable stratification, as has been illustrated using atmospheric observations (Lin, 1969). It is attributed to the flow filed absorbing energy from the scalar temperature field as potential energy is transferred to kinetic

252 energy. It is not clear to what extent near-inertial internal waves contribute in a similar way to
253 spectral redistribution of energy in our oceanographic data.

254 These spectral observations suggest a dominance of convection cascade from sub-
255 meso- via IGW- to, probably because unresolved, turbulence-scales under high-energetic
256 winter-conditions as they show a continuous slope across their frequency ranges. Such a
257 cascade is also suggested under quieter summer conditions when, however, it is masked by
258 IGW that lead a cascade at $\omega > \omega_{min}$. Especially the sub-inertial range of apparent BO-scaling
259 seems out of the turbulence range, unless waters are near-homogeneous $N \rightarrow 0$ so that $\omega_{min} \rightarrow$
260 0. This would extend not only IGW, notably gyroscopic waves, but also turbulence, probably
261 in the form of slantwise convection, to the (sub-)mesoscale range.

262 For the mesoscale range, the observations in Fig. 1 are supported by numerical
263 modeling results that have suggested eddy-KE has a broad range of spectral slopes between -3
264 $< p <$ -5/3 (Storer et al., 2022), and by satellite altimetry observations that indicated, after
265 noise-correction and transfer to KE, a best-fit of $p = -2.28$ (Xu and Fu, 2012). No mention
266 was made of BO-scaling, but the correspondence seems evident.

267 As the KE in Fig. 1 is at least one order of magnitude larger in winter than in
268 summer, a near-inertial peak, if existent, will be part of the spectral continuum during the
269 former. Inspired by Western Mediterranean observations, Saint-Guily (1972) proposed from
270 theoretical work that winter-time inertial KE is spread over a broad featureless band, like
271 quasi-gyroscopic waves that may be present between IGW-bounds $[\omega_{min}, \omega_{max}]$ for $N \sim f$
272 (LeBlond and Mysak, 1978; Gerkema et al., 2008). However, observations from the year-
273 round upper-layer-stratified central Western Mediterranean demonstrate that, also in deep
274 homogeneous $N = 0$ waters, a near-inertial peak is observed in KE-spectra (van Haren and
275 Millot, 2004). This may be attributed to a year-round source of atmospheric-generated inertial
276 waves that are the only internal waves that can propagate without reflection from well-
277 stratified to near-homogeneous layers and back (van Haren, 2023b).

Based on limited spectral observations, Gascard (1973) suggested the generation of 12-h stability waves (close to the buoyancy frequency of very weak stratification) that may briefly force dense-water formation, thereby implicitly suggesting a link between internal waves and (sub-)mesoscale eddies. As such eddies have estimated relative vorticity of $|\zeta| = f/2$ in the Western Mediterranean (Testor and Gascard, 2006), this addition to the planetary vorticity (f) automatically widens the 'effective' near-inertial band $0.5f < f_{eff} < 1.5f$, which bounds are close to IGW-bounds for $N = 0.8f$. One of the properties can be a modification of near-inertial frequency (Perkins, 1976), and trapping with downward propagation of near-inertial waves in anticyclonic eddies (Kunze, 1985; Voet et al., 2024). Such frequency modification may add to local physics of inertial wave caustics due to latitudinal variation (LeBlond and Mysak, 1978), which however can only lead up to 15% change in f in the Mediterranean. Although found to be limited to the rather flat KE-spectral dip in the immediate half-order-of-magnitude sub-inertial frequency band, standing vortical modes (low-frequency non-propagating motions) of vertical length-scale <10 m are suggested to be as energetic as internal waves (Polzin et al., 2003). Alternatively, it has been suggested for North-Atlantic observations that vortical modes may interact with internal waves, affecting internal-wave shear that was peaking over O(10) m vertical scales at IGW-frequencies in a band with limits determined by weak stratification as in $N = f$ (van Haren, 2007).

For hypothetical $\omega_{min} = 0.2$ cpd, at which the observed spectral slope changes away from $p = -11/5$ (Fig. 1), one would require $N = 0.21f$, which is almost unmeasurable and not existent for any prolonged period even in the deep Northwestern Mediterranean, to the knowledge of the author. However, it may reflect ω_{min} computed using $f_{eff} = 0.5f$ and $N = f_{eff}$, noting that such conditions can only apply for part of the record. If so, it would reflect a direct coupling between sub-mesoscale and IGW-motions with slantwise convection (Marshall and Schott, 1999; van Haren and Millot, 2004; Gerkema et al., 2008). The $p = -11/5$ is significantly distinguishable from -2 over a frequency range of nearly two orders of magnitude, and from -5/3 over a range of just over half an order of magnitude (Fig. 1). The

roll-off to noise (slope 0), for $\omega > 5$ cpd, may partially be seen as following a slope of $p = -5/3$ before 0. The roll-off around 0.1 cpd suggests an unresolved broad mesoscale peak-value between 0.01 and 0.1 cpd. While these 1980's moored current meter data barely resolved the turbulence part of the KE-spectrum, and thus also not the p=-5/3 inertial subrange slope, their temperature sensors were too poor to simultaneously verify any spectral scaling for scalars.

About 40 years later, high-resolution moored temperature sensor ''T-' data provided opportunity to verify scalar spectral scaling of turbulence energetic motions in the area. These T-data evidenced occasional warming of the deep Northwest Mediterranean seafloor (Fig. 2a), which, after comparison with data from higher-up appeared to be coming from above, or slanted sideways, under relatively stratified conditions (van Haren, 2023a). The data were collected during mid-fall, when near-surface waters were well stratified and no (cooler) dense-water convection was formed. Locally near the seafloor, the broad two-day warming around day 308 is most stratified, whilst during other periods waters are only weakly stratified, including the quasi-inertial variations between days 316 and 322. These weakly stratified near-inertial, or near-buoyancy as $N \approx f$, temperature variations may evidence slantwise quasi-gyroscopic near-inertial waves, which can have a large vertical component (LeBlond and Mysak, 1978), as opposed to more common near-horizontal near-inertial waves in strongly stratified waters that are barely noticeable in temperature records.

The 18-day average spectra of the 2-s sampled data poorly resolve sub-mesoscales but show a well-resolved slope of $p = -1.4 \pm 0.025$ between $0.5 < \omega < 6000$ cpd, across the IGW band and well into the turbulence band (Fig. 2b). No transition to a -5/3-slope is observed before roll-off to noise, but this does not exclude an inertial subrange at higher frequencies hidden under white noise. The observed $p = -7/5$-slope is found significantly different from $p = -2$ and -5/3 over the indicated frequency range of four orders of magnitude and over the range between $100 < \omega < 10^4$ cpd thereby representing convection turbulence. Over a frequency range of half an order of magnitude the slope-error is about ±0.1. Albeit not greatly resolved, the range between $\omega_{max} < \omega < 10$ cpd falls-off steeper roughly at $p = -2$ and

the range between $10 < \omega < 100$ cpd shows a reduced variance that may partially be characterized by intermittency ($p = -1$; Schuster, 1984), but which is not yet explained. Here, it is observed to bridge between $p = -2$ and super-IGW BO-scaling $p = -7/5$. This would be further observation of a marginally ocean-state to the -1-scaling in KE-spectra (present Fig. 1 and van Haren et al., 2002) and in the continuum of the band [f N] in open-ocean T-spectra (van Haren and Gostiaux, 2009).

Whilst more extended work with longer data sets is to be done, the extended continuous spectral slope from these high-resolution temperature observations suggests a direct coupling between sub-mesoscale motions, IGW motions, comprising internal gravity and gyroscopic waves, and convection turbulence. The temperature spectra also show consistency with the limited KE-spectra of Fig. 1 from roughly the same area, and both indicate a dominance of non-isotropic, stratified-turbulence convection between sub-mesoscales and largest turbulent overturning scales in extended BO-scaling suggesting cross-spectral coupling. The discrepancy with KE-spectra in laboratory experiments of Pawar and Arakeri (2016) may be due to difference of settings. In a non-zero mean flow turbulence convection experiment near the gas-liquid critical point, BO-scaling was observed for both KE and temperature (Ashkenazi and Steinberg, 1999). We recall that our deep-sea conditions are non-zero mean flow, weak tides, very high bulk Reynolds numbers $O(10^5)$ given the large scales, varying non-zero vertical density stratification, and our example spectra did not resolve KO-scaling.

The mesoscale-IGW-turbulence motions transport and locally mix warm waters with cooler surroundings. This contrasts with the process of buoyancy-driven dense-water formation that is thought to bring cooler waters downward during short periods of time, but for which no evidence exists in this 18-day T-sensor data set.

5 How robust is the system of ocean circulation and stratification?

Any variation to the nonlinear system of ocean circulation may encounter several complex feedback mechanisms, of which the effects are not yet fully understood for the

present-day ocean. Although stable density stratification hampers vertical exchange by turbulent mixing, it does not block it. While stratification supports internal waves and their destabilizing shear, turbulent mixing during particular phase of a wave may decrease or destroy it locally in time and space. However, a subsequent internal wave-phase will restratify the mixed patch, thereby maintaining its own support of stable stratification. Such a feedback system may be at work, for example when the ocean absorbs more heat.

Increased sea-surface temperature may lead to increased vertical density stratification, which may lead to less turbulent exchange as vertical overturning is suppressed. However, it will also lead to more internal waves through the extension of their spectral band to higher frequencies, with the potential to increased interaction, non-linearity, and turbulence-generating wave breaking. As particular internal waves can propagate deep into the ocean interior away from their source, they can cause enhanced turbulent mixing elsewhere (e.g., Alford, 2003).

Limited observations have thus far not provided evidence for an inverse correspondence between changes in turbulent mixing and changes in temperature across the near-surface photic zone along a longitudinal section of the Northeast Atlantic Ocean (van Haren at al., 2021b). This lack of correspondence suggests a feedback mechanism at work mediating potential physical environment changes so that global warming may not affect vertical turbulent fluxes of heat, and thereby also of, e.g., carbon. One such feedback mechanism may be (convection-)turbulence induced by internal waves and sub-mesoscale eddies. Re(newed)analysis of yearlong moored current meter data from the Irminger Sea (North-Atlantic Ocean) demonstrate a significant p = -11/5 spectral slope at sub- and at super-inertial frequencies (Fig. 3). As was outlined in van Haren (2007), the area showed an IGW-band (for N = f) with dominant sub-inertial shear at small 8-m vertical scales despite the dominant internal tidal KE. The correspondence with the Mediterranean data of Fig. 1 is striking, including the one order of magnitude change in KE between sub- and super-IGW p = -11/5-slopes with similar p = -1 bridge albeit uncertain crossing level, and similar heights of near-inertial peak despite the tidal peak in Fig. 3.

While few ocean observations have been presented of BO-scaling thus far in comparison with KO-scaling, coupling has not been established between convection and stratified small-scale turbulence with mesoscale motions. Likewise, complicating factors are spectral interruption by internal waves. However, internal wave trapping by mesoscale eddies has been well described (e.g., Kunze, 1985; Voet et al., 2024), and thus provides an obvious coupling between these motions. It is expected that such coupling may lead to strong nonlinearity (of the internal waves) that leads to turbulent mixing produced by wave breaking. Although such turbulent mixing is smaller than that induced by internal wave breaking above sloping topography, such coupling may be an important factor in downward transport of near-inertial energy that eventually breaks elsewhere, e.g., over topography.

As demonstrated using Mediterranean observations, not only convectively unstable cooler and/or saltier waters potentially lead to downward motions from the surface. Also, sub-mesoscale eddies and near-inertial waves can push stratified waters to the deep sea. Such a downward push can be fast to transport materials from surface to 2500-m deep seafloor in a day (van Haren et al., 2006), and which speed is of the same order of magnitude as attributed to dense-water convection (Schott et al., 1996). It can also be more turbulent compared to shear-induced motions in the stratified ocean-interior, whereby turbulence reaches the seafloor according to few observations from the abyssal Pacific (van Haren, 2020) and alpine freshwater Lake Garda (van Haren and Dijkstra, 2021). Further extended observational evidence is urgently needed, preferably resolving much larger scales.

Although the anthropogenic influence on the Earth's climate is without doubt, the impact on ocean circulation is not fully known because we lack sufficient, notably observational, information of the relevant processes that thus cannot be properly modeled yet. Therefore, we should be cautious in making predictions such as in (e.g., Ditlevsen and Ditlevsen, 2023; van Westen et al., 2024) on future ocean circulation based on single parameters like ocean-surface temperature or fresh-water flux that are uncertain proxies. Because no observational (van Haren et al., 2021b), modeling (Little et al., 2020) or paleo-proxy validation (Cisneros et al., 2019) physics evidence exists that sea-surface temperature is

a solid estimator of AMOC-strength variations, other properties like vertical density gradients (stratification), and turbulence intensity may be considered.

Variability of the ocean in space and time is a key to its dynamics, but it is unclear how robust such variations can be, e.g., whether shifting sites for deep dense-water formation (Gou et al., 2024) may be part of the same system. Observational evidence verifying numerical simulations' outcome, not only predictions but also present-day, of ocean-state is needed. Observations are also required to evidence variability in relevant physics processes for model-implementation. Besides eddies and coupling with atmosphere (e.g., Gent, 2018), numerical models of complex nonlinear ocean circulation should contain internal-wave turbulence with appropriate space and time dependency. The importance of (internal wave breaking leading to) boundary mixing (above sloping topography) in general ocean circulation models has been acknowledged in various ways (Scott and Marotzke, 2002; Ferrari et al., 2016).

As for the ocean circulation in the horizontal plane near its surface with most impact on mankind, wind will remain the main driver rather than the AMOC. As long as the Earth rotation does not alter direction, wind will maintain its general course (Wunsch, 2004). The atmosphere remains the key player in the global heat transport across mid-latitudes rather than the ocean. Simultaneously, the importance of processes like stratification and turbulent mixing is induced by, e.g., internal wave breaking with or without sub-mesoscale coupling cannot be underestimated for life near the ocean-surface as well as in the -deep, because it will come to a halt without such processes.

Data availability. No new data were created or analyzed in this study: replot and re-analysis of data presented in van Haren and Millot (2003), van Haren (2007) and van Haren (2023a).

Competing interests. The author declares that he has no conflict of interest.

Acknowledgments. I thank L. Gerringa for commenting on a previous draft of the manuscript.

References

Albérola, C., Millot, C., and Font, J.: On the seasonal and mesoscale variabilities of the Northern Current during the PRIMO-0 experiment in the western Mediterranean Sea. Oceanol. Acta, 18, 163-192, 1995.

Aldama-Campino A., Fransner F., Ödalen, M., Groeskamp, S., Yool, A. Döös, K., and Nycander, J.: Meridional ocean carbon transport, Global Biogeochem. Cy., 34 e2029GB006336, 2023.

Alford, M. H.: Redistribution of energy available for ocean mixing by long-range propagation of internal waves, Nature, 423, 159-162, 2003.

Ashkenazi, S., and Steinberg, V.: Spectra and statistics of velocity and temperature fluctuations in turbulent convection, Phys. Rev. Lett., 83, 4760-4763, 1999.

Bak, P., Tang, C., and Wiesenfeld, K.: Self-organized criticality: An explanation of the 1/f noise, Phys. Rev. Lett., 59, 381-384, 1987.

Bolgiano, R.: Turbulent spectra in a stably stratified atmosphere, J. Geophys. Res., 64, 2226-2229, 1959.

Cisneros, M., Cacho, I., Frigola, J., Snchez-Vidal, A., Calafat, A., Pedrosa-Pàmies, R., Rumín-Caparrós, A., and Canals, M.: Deep-water formation variability in the north-western Mediterranean Sea during the last 2500 yr: A proxy validation with present-day data, Glob. Planet. Chang. 177, 56-68, 2019.

Crepon, M., Wald, L., and Monget, J. M.: Low-frequency waves in the Ligurian Sea during December 1977, J. Geophys. Res., 87, 595-600, 1982.

Ditlevsen, P., and Ditlevsen, S.: Warning of a forthcoming collapse of the Atlantic meridional overturning circulation, Nat. Comm. 14, 4254, 2023.

Emanuel, K., Atmospheric Convection 580 pp., Oxford Univ. Press, New York, 1984.

Eriksen, C. C.: Observations of internal wave reflection off sloping bottoms, J. Geophys. Res., 87, 525-538, 1982.

Ferrari, R., Mashayek, A., McDougall, T. J., Nikurashin, M. and Campin, J.-M.: Turning ocean mixing upside down, J. Phys. Oceanogr., 46, 2229-2261, 2016.

Garrett, C.: The Mediterranean Sea as a climate test basin, In: Malanotte-Rizzoli, P., and Robinson, A. R. eds., Ocean Processes in Climate Dynamics: Global and Mediterranean Examples, Kluwer Academic Publishes, 227-237, 1994.

Garrett, C., and Munk, W.: Space-time scales of internal waves, Geophys. Fluid Dyn., 3, 225-264, 1972.

Gascard, J.-C.: Vertical motions in a region of deep water formation, Deep-Sea Res., 20, 1011-1027, 1973.

Gascard, J-C.: Mediterranean deep water formation, baroclinic eddies and ocean eddies, Oceanol. Acta, 1, 315-330, 1978.

Gent, P. R.: A commentary on the Atlantic meridional overturning circulation stability on climate models, Ocean Mod., 122, 57-66, 2018.

Gerkema, T., Zimmerman, J. T. F., Maas, L. R. M., and van Haren, H.: Geophysical and astrophysical fluid dynamics beyond the traditional approximation, Rev. Geophys., 46, RG2004, doi:10.1029/2006RG000220, 2008.

Gou, R., Wang, Y., Xiao, K., and Wu, L.: A plausible emergence of new convection sites in the Arctic Ocean in a warming climate, Environ. Res. Lett., 19, 031001, 2024.

Gregg, M. C.: Scaling turbulent dissipation in the thermocline, J. Geophys. Res., 94, 9686-9698, 1989.

Hosegood, P., Bonnin, J., and van Haren, H.: Solibore-induced sediment resuspension in the Faeroe-Shetland Channel, Geophys. Res. Lett., 31, L09301, doi:10.1029/2004GL019544, 2004.

Kolmogorov, A. N.: The local structure of turbulence in incompressible viscous fluid for very large Reynolds numbers, Dokl. Akad. Nauk SSSR, 30, 301-305, 1941.

Kunze, E.: Near-inertial wave propagation in geostrophic shear, J. Phys. Oceanogr., 15, 544-565, 1985.

LeBlond, P. H., and Mysak, L. A.: Waves in the ocean, Elsevier, New York, 602 pp., 1978.

Lin, J.-T., Turbulence spectra in the buoyancy subrange of thermally stratified shear flows, 143 pp., PhD-thesis Colorado State University, Fort Collins, 1969.

Little, C. M., Zhao, M., and Buckley, M. W.: Do surface temperature indices reflect centennial-timescale trends in Atlantic Meridional Overturning Circulation strength? Geophys. Res. Lett., 47, e2020GL090888, 2020.

Lohse, D., and Xia, K.-Q.: Small-Scale properties of turbulent Rayleigh-Bénard convection, Annu. Rev. Fluid Mech., 42, 335-364, 2010.

Marotzke, J., and Scott, J. R.: Convective mixing and the thermohaline circulation, J. Phys. Oceanogr., 29, 2962-2970, 1999.

Marshall, J., and Schott, F.: Open-ocean convection: observations, theory, and models, Rev. Geophys., 37, 1-64, 1999.

Mertens, C., and Schott, F.: Interannual variability of deep-water formation in the Northwestern Mediterranean, J. Phys. Oceanogr., 28, 1410-1424, 1998.

Millot, C.: Circulation in the Western Mediterranean Sea, J. Mar. Sys., 20, 423-442, 1999.

Munk, W.: Abyssal recipes, Deep-Sea Res., 13, 707-730, 1966.

Munk, W., and Wunsch, C.: Abyssal recipes II: Energetics of tidal and wind mixing, Deep-Sea Res. I, 45, 1977-2010, 1998.

Obukhov, A. M.: Structure of the temperature field in a turbulent flow, Izv. Akad. Nauk SSSR, Ser. Geogr. Geofiz., 13, 58-69, 1949.

Obukhov, A. M.: Effect of buoyancy forces on the structure of temperature field in a turbulent flow, Dokl. Akad. Nauk SSSR, 125, 1246-1248, 1959.

Pawar, S. S., and Arakeri, J. H.: Kinetic energy and scalar spectra in high Rayleigh number axially homogeneous buoyancy driven turbulence, Phys. Fluids, 28, 065103, 2016.

Perkins, H.: Observed effect of an eddy on inertial oscillations, Deep-Sea Res., 23, 1037-1042, 1976.

Phillips, O. M.: On spectra measured in an undulating layered medium, J. Phys. Oceanogr., 1, 1-6, 1971.

525 Polzin, K. L., Toole, J. M., Ledwell, J. R., and Schmitt, R. W.: Spatial variability of turbulent
526 mixing in the abyssal ocean, Science, 276, 93-96, 1997.
527 Polzin, K. L., Kunze, E., Toole, J. M., and Schmitt, R. W.: The partition of finescale energy
528 into internal waves and subinertial motions, J. Phys. Oceanogr., 33, 234-248, 2003.
529 Reid, R. O.: A special case of Phillips' general theory of sampling statistics for a layered
530 medium, J. Phys. Oceanogr., 1, 61-62, 1971.
531 Rhein, M.: Deep water formation in the western Mediterranean, J. Geophys. Res., 100, 6943-
532 6959, 1995.
533 Saint-Guily, B.: On the response of the ocean to impulse, Tellus 24, 344-349, 1972.
534 Sarkar, S., and Scotti, A.: From topographic internal gravity waves to turbulence, Ann. Rev.
535 Fluid Mech., 49, 195-220, 2017.
536 Schott, F., Visbeck, M., Send, U, Fischer, J., and Desaubies, Y.: Observations of deep
537 convection in the Gulf of Lions, Northern Mediterranean, during the winter of 1991/92, J.
538 Phys. Oceanogr., 26, 505-524, 1996.
539 Schuster, H. G., Determinstc Chaos: An Introduction, Physik–Verlag, Weinheim, 220 pp.,
540 1984.
541 Scott, J. R., and Marotzke, J, 1998: The location of diapycnal mixing and the meridional
542 overturning circulation, J. Phys. Oceanogr., 32, 3578-3595, 2002.
543 Storer, B. A., Buzzicotti, M., Khatri, H., Griffies, S. M., and Aluie, H.: Global energy
544 spectrum of the general oceanic circulation, Nat. Comm., 13, 5314, 2022.
545 Taira, K., Yanagimoto D., and Kitagawa, S.: Deep CTD casts in the challenger deep. Mariana
546 Trench, J. Oceanogr., 61, 447-454, 2005.
547 Testor, P., and Gascard, J.C.: Post-convection spreading phase in the Northwestern
548 Mediterranean Sea, Deep-Sea Res., 53, 869-893, 2006.
549 Thorpe, S. A.: Transitional phenomena and the development of turbulence in stratified fluids:
550 a review, J. Geophys. Res., 92, 5231-5248, 1987.
551 van Haren, H.: Inertial and tidal shear variability above Reykjanes Ridge, Deep-Sea. Res. I,
552 54, 856-870, 2007.

553 van Haren, H.: Slow persistent mixing in the abyss, Ocean Dyn., 70, 339-352, 2020.
554 van Haren, H.: Convection and intermittency noise in water temperature near a deep
555 Mediterranean seafloor, Phys. Fluids, 35, 026604, 2023a.
556 van Haren, H.: Near-inertial wave propagation between stratified and homogeneous layers, J.
557 Oceanogr., 79, 367-377, 2023b.
558 van Haren, H., and Dijkstra, H. A.: Convection under internal waves in an alpine lake, Env.
559 Fluid Mech., 21, 305-316, 2021.
560 van Haren, H., and Gostiaux, L.: High-resolution open-ocean temperature spectra, J.
561 Geophys. Res., 114, C05005, doi:10.1029/2008JC004967, 2009.
562 van Haren, H., and Gostiaux, L.: Detailed internal wave mixing observed above a deep-ocean
563 slope, J. Mar. Res., 70, 173-197, 2012.
564 van Haren, H. and Millot, C.: Seasonality of internal gravity waves kinetic energy spectra in
565 the Ligurian Basin, Oceanol. Acta, 26, 635-644, 2003.
566 van Haren, H., and Millot, C.: Rectilinear and circular inertial motions in the Western
567 Mediterranean Sea, Deep-Sea Res. I, 51, 1441-1455, 2004.
568 van Haren, H., Maas, L., and van Aken, H.: On the nature of internal wave spectra near a
569 continental slope, Geophys. Res. Lett., 29(12), 10.1029/2001GL014341, 2002.
570 van Haren, H., Millot, C., and Taupier-Letage, I.: Fast deep sinking in Mediterranean eddies,
571 Geophys. Res. Lett., 33, L04606, doi:10.1029/2005GL025367, 2006.
572 van Haren, H., Ribó, M., and Puig, P.: (Sub-)inertial wave boundary turbulence in the Gulf of
573 Valencia. J. Geophys. Res.Oceans, 118, 2067-2073, doi:10.1002/jgrc.20168, 2013.
574 van Haren, H., Uchida, H., and Yanagimoto, D.: Further correcting pressure effects on
575 SBE911 CTD-conductivity data from hadal depths, J. Oceanogr., 77, 137-144, 2021a.
576 van Haren, H., Brussaard, C. P. D., Gerringa, L. J. A., van Manen, M. H., Middag, R., and
577 Groenewegen, R.: Diapycnal mixing near the photic zone of the NE-Atlantic, Ocean Sci.,
578 17, 301-318, 2021b.

van Haren, H., Voet, G., Alford, M. H., Fernandez-Castro, B., Naveira Garabato, A. C., Wynne-Cattanach, B. L., Mercier, H., and Messias, M.-J.: Near-slope turbulence in a Rockall canyon, Deep-Sea Res. I, 206, 104277, 2024.

van Westen, R. M., Kliphuis, M., and Dijkstra, H.A.: Physics-based early warning signal shows that AMOC is on tipping course, Sci. Adv., 10, eadk1189, 2024.

Voet, G., et al.: Near-inertial energy variability in a strong mesoscale eddy field in the Iceland Basin, Oceanogr., 37, https://doi.org/10.5670/oceanog.2024.302, 2024.

Winters, K. B.: Tidally driven mixing and dissipation in the stratified boundary layer above steep submarine topography, Geophys. Res. Lett., 42, 7123-7130, 2015.

Wunsch, C.: Gulf Stream safe if wind blows and Earth turns, Nature, 428, 601, 2004.

Wunsch, C., and Ferrari, R.: Vertical mixing, energy and the general circulation of the oceans, Ann. Rev. Fluid Mech., 36, 281-314, 2004.

Wynne-Cattanach, B. L., Couto, N., Drake, H. F., Ferrari, R., Le Boyer, A., Mercier, H., Messias, M.-J., Ruan, X., Spingys, C. P., van Haren, H., Voet, G., Polzin, K., Naveira Garabato, A., and Alford, M. H.: Observational evidence of diapycnal upwelling within a sloping submarine canyon, Nature, 630, 884-890, 2024.

Xu, Y., and Fu, L.-L.: The effects of altimeter instrument noise on the estimation of the wavenumber spectrum of sea surface height, J. Phys. Oceanogr., 42, 2229-2233, 2012.

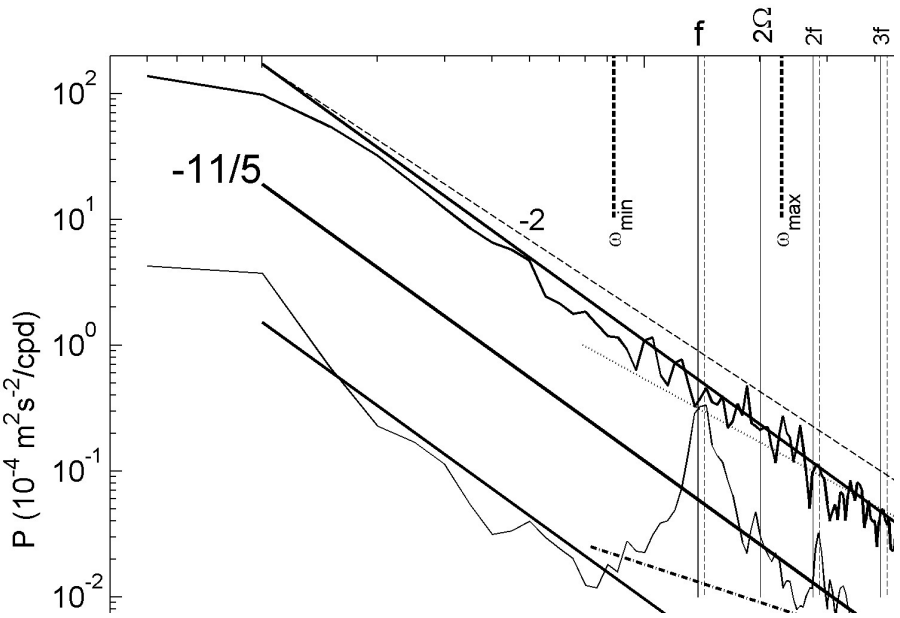

Fig. 1. Moderately smoothed (20 degrees of freedom, dof) kinetic energy (KE) spectra over 100 days of data from 600-s sampled Aanderaa mechanical current meter moored in 1981/1982 at z = -1100 m over the continental slope in the Ligurian Sea at 43° 28.32′ N, 7° 46.10′ E, 2250 m water depth. For details on these data, see van Haren and Millot (2003). The 'summer' spectrum is an average from data between days 190 and 290 (in 1981), the 'winter' between days 375 and 475 (adding +365 for days in 1982). Several frequencies are indicated including inertial frequency f, Earth rotational Ω and inertio-gravity wave bounds [ω_{min}<f, ω_{max}>N] for buoyancy frequency N = f. The dashed lines indicate (harmonics of) 1.04f. Four spectral slopes ω^p are indicated by their exponent: p = -11/5 (solid slope in the log-log plot) for Bolgiano-Obukhov 'BO' scaling reflecting the buoyancy subrange of convective turbulence (e.g., Pawar and Arakeri, 2016), p = -5/3 (dotted slope) for Kolmogorov-Obukhov 'KO' scaling reflecting the equilibrium inertial subrange for dominant shear-induced turbulence (Kolmogorov 1941; Obukhov, 1949), p = -1 (dash-dotted slope) for intermittency of self-organized criticality (Schuster, 1984; Bak et al., 1987) and p = -2 (dashed slope) for internal wave scaling (Garrett and Munk, 1972) or finestructure contamination (Phillips, 1971; Reid, 1971).

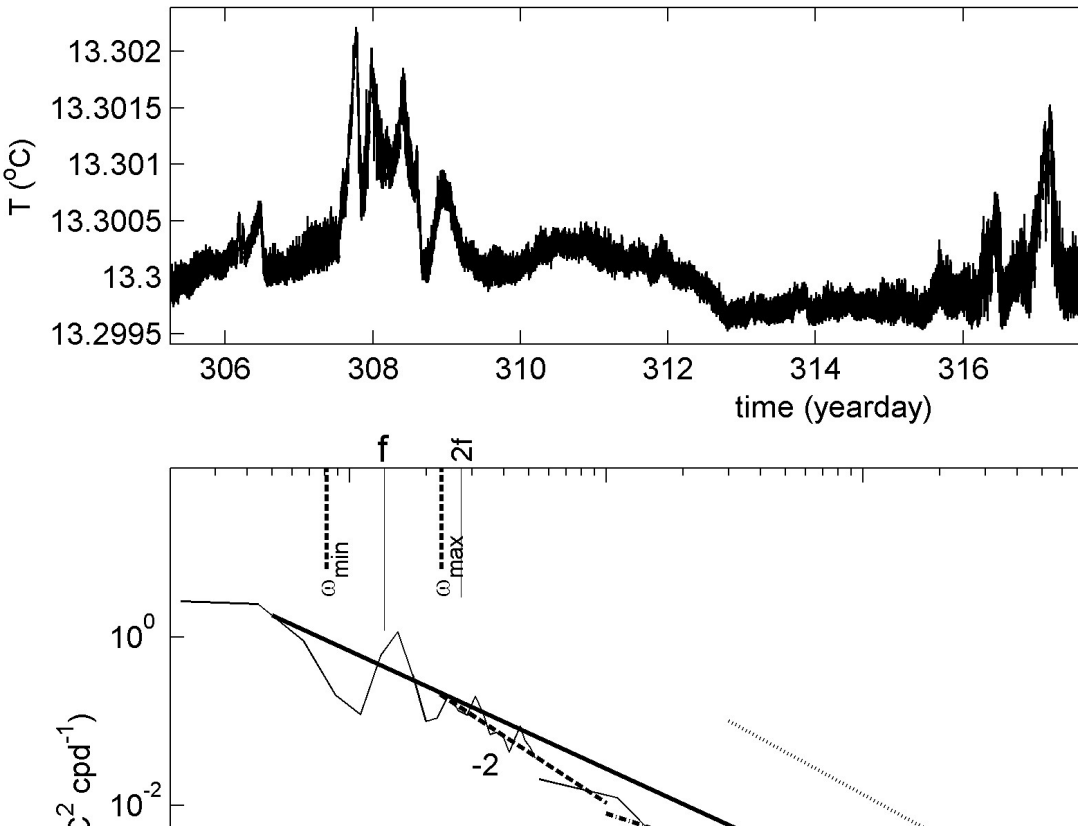

Fig. 2. Eighteen days of high-resolution 2-s sampled temperature (T) data from a NIOZ T-sensor fallen off a mooring-line in 2020 and lying 0.01 m above a flat seafloor about 10 km south of the foot of the continental slope at 42° 49.50′ N, 6° 11.78′ E, 2458 m water depth, about 100 km WSW from the site in Fig. 1. For details on these data see van Haren (2023a). (a) Time series of 18 days of raw temperature data. (b) Weakly smoothed (10 dof; ω<5 cpd) and heavily smoothed (250 dof; ω>5 cpd) temperature variance spectra of data in a. Frequency and spectral slope indications as in Fig. 1, while -7/5 (solid slope) indicates BO-scaling of an active scalar (e.g. Pawar and Arakeri, 2016), and -1 (dash-dotted slope) for scaling of intermittency of a weakly chaotic nonlinear system (Schuster, 1984). Note the different axes-ranges compared with Fig. 1.

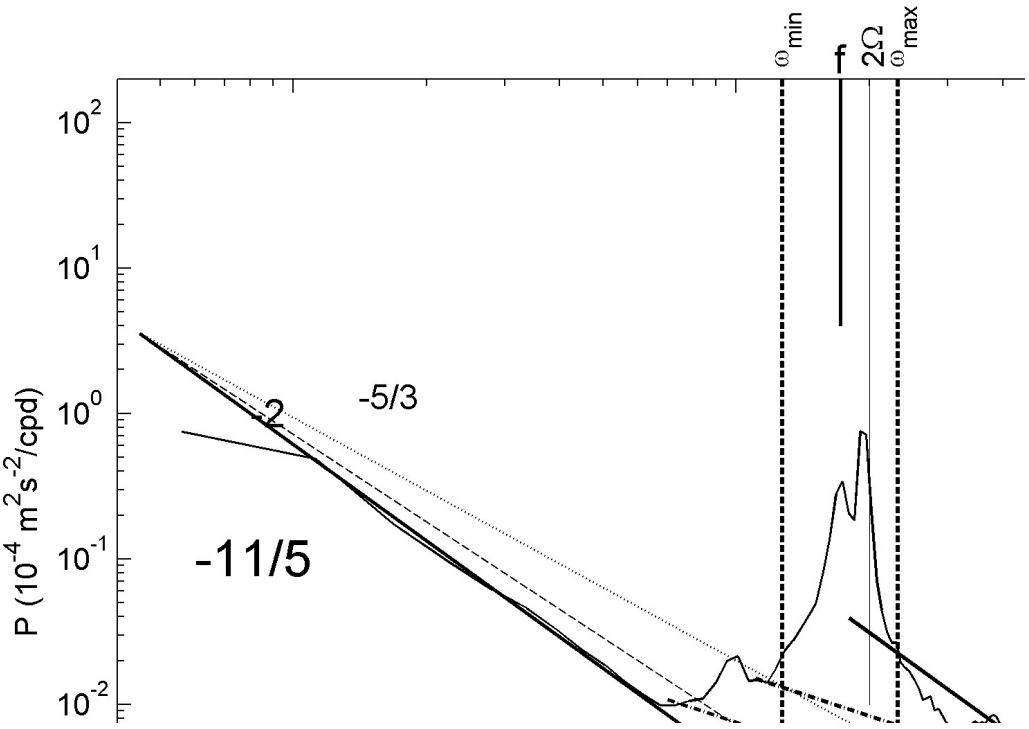

Fig. 3. Like Fig. 1, but for strongly smoothed (50 dof) KE spectra averaged over 400 days of data from 600-s sampled Valeport mechanical current meter moored at z = -1000 m over the Mid-Atlantic Ridge at 58° 59.67′ N, 33° 56.12′ W, 2540 m water depth in 2003/2004, within the project discussed in van Haren (2007).